

Resonance energy transfer: Influence of neighboring matter absorbing in the wavelength region of the acceptor

David L. Andrews and Jack S. Ford

Citation: *J. Chem. Phys.* **139**, 014107 (2013); doi: 10.1063/1.4811793

View online: <http://dx.doi.org/10.1063/1.4811793>

View Table of Contents: <http://jcp.aip.org/resource/1/JCPSA6/v139/i1>

Published by the AIP Publishing LLC.

Additional information on J. Chem. Phys.

Journal Homepage: <http://jcp.aip.org/>

Journal Information: http://jcp.aip.org/about/about_the_journal

Top downloads: http://jcp.aip.org/features/most_downloaded

Information for Authors: <http://jcp.aip.org/authors>

ADVERTISEMENT

physicstoday

Comment on any
Physics Today article.

Physics Today / Volume 63 / Issue 7 / July 2012
Previous Article | Next Article

Measured energy in Japan
David von Seggern
(dvs@seismo.unr.edu) University of Nevada
July 2012, page 10
DIGITAL OBJECT IDENTIFIER
<http://dx.doi.org/10.1063/PT.3.1619>

The article by Thorne Lay and Hiroo Kanamori (10.1063/PT.3.1619) is an excellent review of the energy released by the 11-Megaton atomic bombing of Nagasaki in 1945. The authors estimate that the energy released was approximately five times as much energy as that of a 30-megaton nuclear detonation event—a 30-megaton atmospheric event. The 1964 Chilean earthquake had still more energy by a factor of about 3, or 15 times as much energy as that of a 30-megaton nuclear device. I believe the authors used the relation for seismic energy release rather than total strain energy release. The seismic energy underestimates the total strain energy release by a variable that depends on the fault plane. Accounting for total strain energy release would increase the earthquake energy number by orders of magnitude.

Despite the catastrophic damage potential of nuclear bombs, the forces of nature occasionally unleash much larger energy releases. Although the nuclear bombs are under our control, earthquakes, volcanic eruptions, and extreme weather events are not. However, by judicious preparation and avoidance measures, humans can significantly diminish the damage of natural events.

This article does not have any references.

Comment on this article
By the act of hitting a ball with a bat, one calculates the force energy to deliver the ball to its new location, but one must also take into account that the ball extended its energy release to that which became struck by the ball as its momentum ceased and passed energy to the struck team. Therefore the parameters of the damage extend into the future when the received energy to that pushed upon, later becomes released in a new event. Perhaps calculations of one added that in while another's calculations did not. E.M.C.
Written by Edgar Mocarvill, 14 July 2012 19:59

Resonance energy transfer: Influence of neighboring matter absorbing in the wavelength region of the acceptor

David L. Andrews^{a)} and Jack S. Ford

School of Chemistry, University of East Anglia, Norwich Research Park, Norwich NR4 7TJ, United Kingdom

(Received 18 April 2013; accepted 10 June 2013; published online 2 July 2013)

In many of the materials and systems in which resonance energy transfer occurs, the individual chromophores are embedded within a superstructure of significantly different chemical composition. In accounting for the influence of the surrounding matter, the simplest and most widely used representation is commonly cast in terms of a dependence on local refractive index. However, such a depiction is a significant oversimplification, as it fails to register the electronic and local geometric effects of material specifically in the vicinity of the chromophores undergoing energy transfer. The principal objective of this study is to construct a detailed picture of how individual photon interaction events are modified by vicinal, non-absorbing chromophores. A specific aim is to discover what effects arise when input excitation is located in the neighborhood of other chromophores that have a slightly shorter wavelength of absorption; this involves a passive effect exerted on the transfer of energy at wavelengths where they themselves display no significant absorption. The theory is based on a thorough quantum electrodynamical analysis that allows the identification of specific optical and electronic chromophore attributes to expedite or inhibit electronic energy transfer. The Clausius-Mossotti dispersion relationship is then deployed to elicit a dependence on the bulk refractive index of the surroundings. A distinction is drawn between cases in which the influence on the electromagnetic coupling between the donor and the acceptor is primarily due to the static electric field produced by a polar medium, and converse cases in which the mechanism for modifying the form of energy transfer involves the medium acquiring an induced electric dipole. The results provide insights into the detailed quantum mechanisms that operate in multi-chromophore systems, pointing to factors that contribute to the optimization of photosystem characteristics. © 2013 AIP Publishing LLC. [<http://dx.doi.org/10.1063/1.4811793>]

I. INTRODUCTION

This study concerns the effect of molecules near specific light-absorbing chromophores, on the transfer of electronic excitation in a complex multi-component molecular system. At the molecular level, the effects of such components, not specifically absorbing in the same wavelength region as the excitation donor or acceptor, can be understood in terms of their electronic polarizability. Molecular polarizability is a tensor quantity with elements whose dispersion character, owing to an intricate dependence on transition energies and dipoles, typically exhibit their largest and most sharply wavelength-dependent values at near-resonant wavelengths. Accordingly, appropriately positioned components can significantly modify the strength of electromagnetic influence in their vicinity, and this effect can modify the character of a nearby energy transfer process. It is well known that polarizability values are related to refractive index by the Clausius-Mossotti equation, affording the basis for linkage to a description in terms of bulk properties of the medium. Here, one can begin to consider the net effect of all the matter comprising the system in statistical terms, such as compositional fractions. Although expedient, the application of such bulk concepts to processes that fundamentally involve photonic interactions is

decidedly crude. In materials where chromophores of a variety of types form local arrangements of complex architecture, it can reasonably be supposed that the detailed quantum mechanisms operating at the local chromophore-photon level might operate in a fashion significantly different from that predicted for the bulk.

Our principal aim is to construct a detailed picture of how individual photon interaction events are modified by vicinal, non-absorbing chromophores. We seek to discover what particular effects arise when input excitation is located in the neighborhood of other, constitutionally different chromophores that have a slightly shorter wavelength absorption – sufficiently removed from the wavelength equivalent of the transfer energy to obviate direct action as a third body absorber, as illustrated in Figure 1.

This is indeed a situation that arises in many photosynthetic systems.¹ It is well known that chromophores absorbing at short wavelengths, absorbing from a broadband input, commonly harvest energy and transfer it with minor losses to other, longer-wavelength absorbers. There are also ancillary pigments that have significant photoprotective roles associated with direct absorption.² However, our concern is with the passive effect that such species can exert on the transfer of energy at wavelengths where they themselves display no significant absorption. The results can provide insights into the detailed quantum mechanisms that operate in

^{a)} Author to whom correspondence should be addressed: david.andrews@physics.org

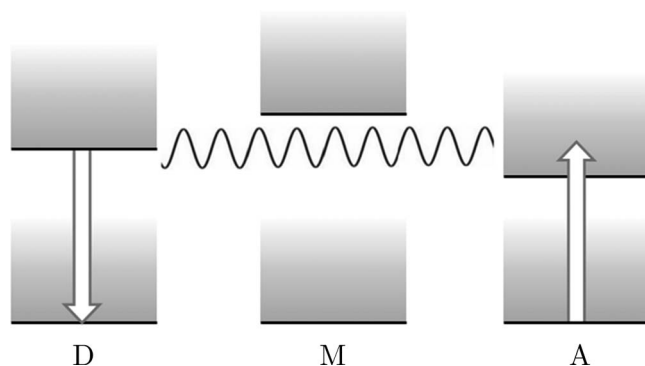


FIG. 1. Schematic Jablonski-type depiction of an energy transfer between donor D and acceptor A, in the vicinity of a species M with a higher first excited state.

multi-chromophore systems, pointing to factors that contribute to the optimization of photosystem characteristics. As Scholes *et al.*³ have pointed out, energy harvesting efficiency is generally determined by the interplay of numerous factors.

An example serves to illustrate the cases we shall consider. Natural photosystems generally contain a proliferation of chromophores with absorption bands shifted to differing extents by local molecular structure. In many photobacterial systems based on bacteriochlorophyll B800 and B850 (the numerals denoting absorption maxima in nanometers), it is well understood that B800 chromophores commonly absorb light of this wavelength and then pass excitation on to a B850, when both are in the same vicinity.⁴ The corresponding spectroscopic gradient,⁵ which is offset by minor vibrational losses, serves to impart a significant degree of directionality to the energy routing. Although it might be supposed that replacing the B800 with B850 might achieve the same end in a system of reduced complexity, higher densities of B850 could promote singlet-singlet annihilation and exciton formation. So, given the naturally occurring local architecture one can pose the question; is there an effect on the transfer of energy, following absorption of 800 nm radiation by B800, to B850? Seminal work by Scholes and Fleming⁶ has considered in detail the dielectric influence of surrounding protein host material, as well as the mutual interaction of the donor and acceptor. Nonetheless, the density of chromophore packing in such structures suggests the possibility of other, additional effects due to non-participant bacteriochlorophyll units, those not directly engaged as donor or acceptor. Such questions are only indicative of the much broader issues which we now turn to address.

Although the analysis has particular relevance to the role of ancillary pigments in photobiological systems, the principles to be established will have a wider application to various forms of complex structured materials. Accordingly, this work is intended as part of a larger study aiming to determine the key principles for optimizing the sought photonic mechanisms in meta-structured molecular materials, through the inclusion of suitable chromophores. In the design of functional optical materials, there is currently great interest in deploying the mechanism of internal electronic energy transport to achieve or enhance desired photophysical characteristics.⁷ A primary area of application can be found in the field of arti-

ficial energy harvesting materials, but numerous other examples arise in nonlinear optical connections.^{8–11} The identification of stepwise energy transfer mechanisms in natural photosynthetic systems, typically following an initial absorption of light, has inspired efforts to secure similar principles of operation in molecular nanomaterials.^{12,13} Examples are readily found in the realm of dendrimers and other self-assembled molecular structures such as block copolymers.^{14–16} Energy transport between electronically distinct components or chromophores within such systems usually operates as a multi-step sequence, due to the sharp decline in efficiency with distance. Each stage is an ultrafast migration that is well described by the standard Förster model¹⁷ of resonance energy transfer (RET).

Molecular quantum electrodynamics (QED) has been widely and very successfully applied to such processes, producing a unified theory that reconciles both RET and radiative energy transfer as the short- and long-range limits of one mechanism.^{18–21} The purpose of the present analysis is to address this problem using a more rigorous approach to the representation of local molecular electronic structure. In the following, by developing a thorough quantum electrodynamical analysis including state-sequence methodology, extending a recent analysis by Salam,²² a path is established towards a formalism that will allow the identification of specific optical and electronic chromophore attributes to expedite or inhibit electronic energy transfer.

II. QED BACKGROUND

A. Foundations

To fully describe the coupling of donor relaxation and acceptor excitation events involved in RET (excluding exchange via molecular wavefunction overlap), a quantum electrodynamical treatment is required. QED is an essential framework for rigorous analysis of the interactions of molecules with light, and their electromagnetic interactions with each other.^{23,24} Quantizing the whole system under consideration, particles and fields alike, introduces the virtual photon for describing the couplings between particles of matter;^{20,23} this ensures that causality and retardation principles are inbuilt. In fact, where molecules are not in direct contact, all intermolecular interactions must be mediated by virtual photon exchange. For each molecule, every discrete electronic transition is a local matter-radiation interaction event.

The non-relativistic Hamiltonian operator for a system comprised of interacting molecules ξ , promoted to operator form, is exactly expressible as

$$H = H_{\text{radiation}} + \sum_{\xi} H_{\text{matter}}(\xi) + \sum_{\xi} H_{\text{interaction}}(\xi). \quad (1)$$

Since the theory that is to be developed from this basis will have wide-ranging general validity, the terms “molecule” and “chromophore” can be regarded as essentially interchangeable in the following. Operations of the interaction Hamiltonian term, henceforth abbreviated as H_{int} , account for individual transition events within each interacting molecule. The rate (probability per unit time), Γ_{FI} , of an identified transition process is given by the Fermi golden rule.²⁵ For a

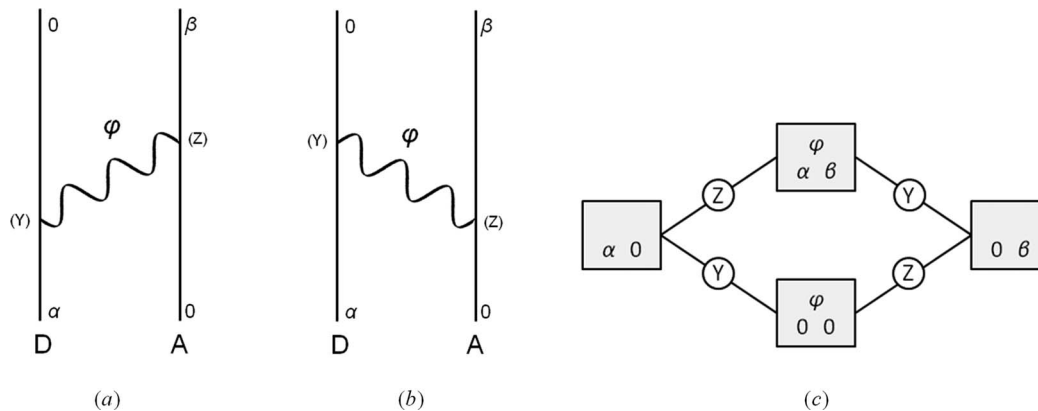


FIG. 2. RET. Event (Y) is the relaxation of D, event (Z) the excitation of A. The Feynman diagrams show the time-order: (a) (Y) \rightarrow (Z); (b) (Z) \rightarrow (Y). The state-sequence diagram (c) contains all the information of both Feynman diagrams. Reproduced by permission from D. L. Andrews and J. S. Ford, Proc. SPIE **8459**, 84590C (2012). Copyright 2012 SPIE.

system proceeding from its initial state I to a final state F within a continuum of density ρ_F ,

$$\Gamma_{FI} = 2\pi \hbar^{-1} \rho_F |M_{FI}|^2. \quad (2)$$

A process consisting of N interaction events is described by Nth-order perturbation theory, such that its quantum amplitude M_{FI} is given by the Nth term of the perturbation expansion,²⁶

$$M_{FI} = \langle F | H_{\text{int}} | I \rangle + \sum_R \frac{\langle F | H_{\text{int}} | R \rangle \langle R | H_{\text{int}} | I \rangle}{(E_I - E_R)} + \sum_{R,S} \frac{\langle F | H_{\text{int}} | S \rangle \langle S | H_{\text{int}} | R \rangle \langle R | H_{\text{int}} | I \rangle}{(E_I - E_R)(E_I - E_S)} + \dots \quad (3)$$

The analysis of electronic energy transport concerns the exchange of quanta between discrete chromophores individually possessing characterized absorption and fluorescence. For example, elementary absorption entails the annihilation of single photons, and is accordingly represented by the first order term in Eq. (3). In its simplest form, RET entails one donor and one acceptor, the mechanism for energy transfer being described as the exchange of a single virtual photon. Here, since there is one photon creation and a corresponding photon annihilation event, the leading term in the theory emerges from the second order term in Eq. (3). When the donor and acceptor chromophores are embedded within a host medium comprising optically passive molecules, the influence upon RET is described by considering the passive electromagnetic influence of a neighboring chromophore upon each absorber, or each interacting pair. Once again, the only mechanism for exerting such an influence is virtual photon coupling, for which the associated creation and annihilation events add two to the order of the term in Eq. (3) that leads. Accordingly, fourth order perturbation theory forms the basis for identifying passive chromophore effects on RET.

B. Coupling configurations and their diagrammatic representations

Intermolecular interaction processes are understood by this formalism to consist of molecules changing their elec-

tronic states while exchanging photons. Equation (3) sums all the quantum amplitude results that involve the accessible system intermediate states R, S, etc. A process consisting of multiple interaction events may proceed with those events occurring in any order, and each time-ordering involves the system transitioning through a unique sequence of intermediate states. Each such time-ordering may be illustrated by plotting the positions of the molecules and photons in nonrelativistic Feynman diagrams, where the vertical dimension proceeding upward signifies time and the horizontal dimension represents a spatial direction. Since each Feynman diagram illustrates one time-ordering, $N!$ such Feynman diagrams are required to account for all $N!$ permutations of the N interaction events. Whereas the Feynman diagrams represent each fundamental photon interaction as a vertex and states as line segments, there is an alternative graphical form in which the states are cast as vertices on a net in which the interactions form the edges. Such state-sequence representations²⁷ (equivalent to Hasse diagrams²⁸ with superior elements to the right) have the advantage of accommodating the full information content of all $N!$ time-ordered graphs.

In the case of RET between a donor chromophore D and counterpart acceptor A, the transfer of electronic excitation via virtual photon may be illustrated with the two Feynman diagrams shown in Fig. 2. The donor relaxes from an initial excited state α to its ground state 0 in event (Y); the acceptor is excited by an equal amount from its ground state to its state β in event (Z). Figure 2 illustrates the two time-orderings, and the corresponding state-sequence diagram accounting for both.²⁷

The exchange of an additional photon p with a passive chromophore M is the lowest-order coupling process that elevates RET to third-body-modified RET. Figure 3 shows one configuration, where it is chromophore D that interacts with both photons, through which the three-chromophore system may connect together. Later in the present analysis, the theory will be extended and generalized to subsume this particular case. The four distinct matter-radiation interaction events are labeled (W), (X), (Y), and (Z). At each event, one molecule undergoes a transition between states 0, α , r , β and one photon is either created or annihilated.

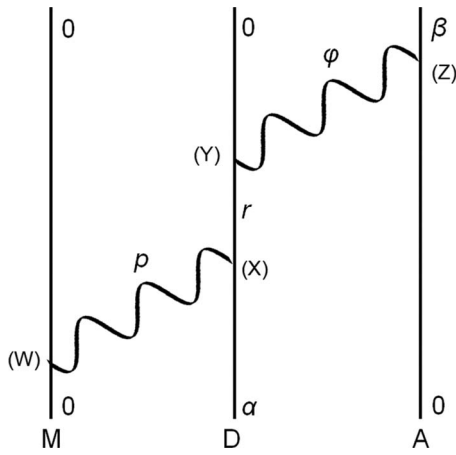


FIG. 3. One time-ordering for one coupling configuration for third-body-modified RET. Event (W) is the static interaction of M, (X) is the interaction of D with photon p , (Y) is the interaction of D with photon ϕ , and (Z) the excitation of A. Reproduced by permission from D. L. Andrews and J. S. Ford, Proc. SPIE **8459**, 84590C (2012). Copyright 2012 SPIE.

The four events may occur in any time-ordering, such that there are $4! = 24$ permutations. Therefore, 23 other Feynman diagrams may be constructed which equally describe the same overall process, which we shall refer to as the MDA configuration – signifying by shorthand the photon connectivity of the three components (not necessarily their geometric alignment). An initial treatment of this feature was given in Ref. 29; the present system-based approach will afford a more detailed investigation of the electrodynamic involvement of the donor-acceptor pair with its material surroundings.

The occurrence of four transition events punctuates five stages of the system's evolution, labeled I, R, S, T, F in chronological order. In each stage, there are various possible states that the overall system may occupy, depending on the particular event-ordering – i.e., which of the 24 Feynman diagrams is being followed. This corresponds to the summations over system states in Eq. (3). Figure 4 expresses the system's evolution through the five stages with one state-sequence diagram that summarizes the impacts of the four events in every time-order. Each of the 24 pathways through the state-sequence network represents one event-ordering, formally a

mapping of one of the Feynman diagrams. For example, Fig. 3, illustrating the process with (W)→(X)→(Y)→(Z) ordering, corresponds to the uppermost pathway in Fig. 4.

The state-sequence network has precisely the form of a four-dimensional hypercube,²⁷ with states as vertices and events as cell edges. The combinatorial possibilities of four transitions occurring in any order map to a representation of a four-dimensional state space, through which the system moves in unit vector leaps from I to the opposing vertex F of this hypercube.

III. QUANTUM AMPLITUDES

A. Derivation for the MDA coupling configuration

Applying the electric dipole approximation, the interaction Hamiltonian operator for each event takes the form $(-\epsilon_0^{-1})\boldsymbol{\mu} \cdot \mathbf{d}^\perp$. From the standard mode expansion²³ for the electric displacement field operator \mathbf{d}^\perp , when applied to a radiation mode of wavevector \mathbf{p} , it emerges that an interaction taking the molecule from state A to state B corresponds to the following Dirac bracket:

$$\begin{aligned} \langle B | H_{\text{int}} | A \rangle &= -i\mu_i^{BA} \sum_{\mathbf{p}e_{(\mathbf{p})}} \left(\frac{\hbar c p}{2\epsilon_0 V} \right)^{1/2} \\ &\times (e_{(\mathbf{p})i} \exp(i\mathbf{p} \cdot \mathbf{r}) \langle rad_B | a_{\mathbf{p}} | rad_A \rangle \\ &- \bar{e}_{(\mathbf{p})i} \exp(-i\mathbf{p} \cdot \mathbf{r}) \langle rad_B | a_{\mathbf{p}}^\dagger | rad_A \rangle). \end{aligned} \quad (4)$$

The subscript i is a Cartesian index that relates the direction of the molecule's transition dipole moment vector to that of the radiation mode's polarization vectors $\mathbf{e}_{(\mathbf{p})}$, using the convention of implied summation over repeated tensor indices: overbars denote complex conjugation. The vector \mathbf{r} is the molecular position, $a_{\mathbf{p}}$ and $a_{\mathbf{p}}^\dagger$ are, respectively, the photon annihilation and creation operators for radiation mode \mathbf{p} , and V is the arbitrary volume of quantization.

For any particular time-ordering of the four interaction events, the quantum amplitude of the MDA configuration of third-body-modified RET is given by the fourth term of Eq. (3). Hence, we obtain

$$\begin{aligned} M_{FI} &= \sum_{R,S,T} \frac{\langle F | H_{\text{int}} | T \rangle \langle T | H_{\text{int}} | S \rangle \langle S | H_{\text{int}} | R \rangle \langle R | H_{\text{int}} | I \rangle}{[E_{IT}^D + E_{IT}^A - E_T^{\text{rad}}][E_{IS}^D + E_{IS}^A - E_S^{\text{rad}}][E_{IR}^D + E_{IR}^A - E_R^{\text{rad}}]} \\ &= \left(\frac{\hbar c}{2\epsilon_0 V} \right)^2 \sum_{\mathbf{p}, e_{(\mathbf{p})}, \phi, e_{(\phi)}} \frac{p\phi \bar{e}_{(\mathbf{p})a} e_{(\mathbf{p})b} \bar{e}_{(\phi)c} e_{(\phi)d} \mu_i^{M_o M_o} \mu_j^{D_o D_r} \mu_k^{D_r D_o} \mu_l^{A_\beta A_o}}{[E_{\alpha T}^D + E_{0T}^A - E_T^{\text{rad}}][E_{\alpha S}^D + E_{0S}^A - E_S^{\text{rad}}][E_{\alpha R}^D + E_{0R}^A - E_R^{\text{rad}}]} \\ &\times \exp(i\mathbf{p} \cdot (\mathbf{r}_{p\text{Ann.}} - \mathbf{r}_{p\text{Cre.}}) + i\phi \cdot (\mathbf{r}_{\phi\text{Ann.}} - \mathbf{r}_{\phi\text{Cre.}})), \end{aligned} \quad (5)$$

where $E_{AB} \equiv E_A - E_B$. In each case, these variables are specified by the states explicitly labeled in the boxes of the state-sequence diagram of Fig. 4, e.g., the E^{Rad} terms will deliver

0 , $\hbar c p$, $\hbar c \phi$, or $\hbar c(p + \phi)$. The \mathbf{r} vectors of Eq. (5) are the positions of the interaction events that create and annihilate the photons p and ϕ . The variables p and ϕ are the magnitudes

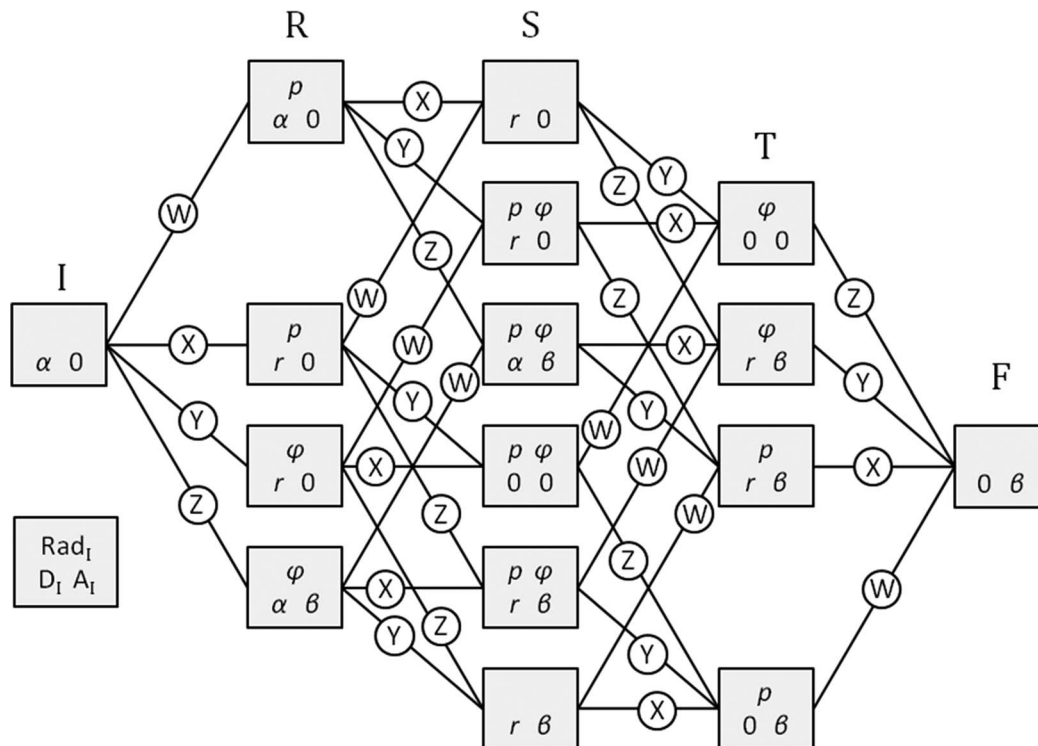


FIG. 4. State-sequence diagram for the MDA configuration of third-body-modified RET. Time progresses left to right, each of the 16 boxes representing one of the possible overall states of the system in one of the five stages I, R, S, T, F . Each overall state comprises states for each changing sub-system – the radiation, and chromophores D and A . In each system state, M remains in its ground state. Reproduced by permission from D. L. Andrews and J. S. Ford, Proc. SPIE **8459**, 84590C (2012). Copyright 2012 SPIE.

of wavevectors \mathbf{p} and $\boldsymbol{\phi}$. The new spatial indices a, b, c, d describe directional information for the radiation polarizations. Each relates to the directionality of the transition dipole moment associated with the photon's creation/annihilation, such that a, b, c, d represent some permutation of i, j, k, l determined by which molecular transition creates or annihilates each photon.

Equation (5) is the quantum amplitude for energy transfer within a finite volume of quantization V , via a particular event-order. The general result for energy transfer at the limit of infinite V , with the time-ordering of events left unspecified, is found by recasting the sum over modes \mathbf{p} and $\boldsymbol{\phi}$ as triple integrations over \mathbf{p} -space and over $\boldsymbol{\phi}$ -space. The sum over all 24 event-orderings yields

$$\begin{aligned}
 M_{FI} &= (2\pi)^{-2} (2\epsilon_0)^{-2} \mu_a^{M_a M_o} \mu_d^{A_\beta A_o} \sum_{D_r} \left\{ \frac{\mu_b^{D_o D_r} \mu_c^{D_r D_a}}{E_{\alpha r}^D} + \frac{\mu_c^{D_o D_r} \mu_b^{D_r D_a}}{E_{\alpha r}^D - \hbar c k} \right\} \\
 &\times (\nabla^2 \delta_{ab} - \nabla_a \nabla_b) R_{MD}^{-1} (\nabla'^2 \delta_{cd} - \nabla'_c \nabla'_d) R_{DA}^{-1} \exp(ik R_{DA}) \\
 &\because \mathbf{R}_{AB} \equiv \mathbf{r}_A - \mathbf{r}_B; \quad \nabla_j \equiv \partial/\partial R_{MDj}; \quad \nabla'_j \equiv \partial/\partial R_{DAj}.
 \end{aligned} \tag{6}$$

Hereafter, k refers specifically to the wavenumber $k \equiv E_{\alpha 0}^D/\hbar c = E_{\beta 0}^A/\hbar c$. All variables associated with \mathbf{p} and $\boldsymbol{\phi}$ have been eliminated, as the photons are considered virtual and all possible values of their wave-vectors are accommodated. This is the result for the MDA configuration quantum amplitude.

For a generic chromophore X , the specific form of linear polarizability for the transition $X_f \leftarrow X_0$ is given

by implementation of the standard result for a generalized and damped polarizability tensor, as given in Eq. (7) below. This describes any process in which the molecule X undergoes this state transition via unspecified intermediate state r , entailing one photon absorption and one photon emission. The wavenumbers k and k' are those of the input and output photons, respectively. The wavenumber γ_r^X represents damping, incorporated

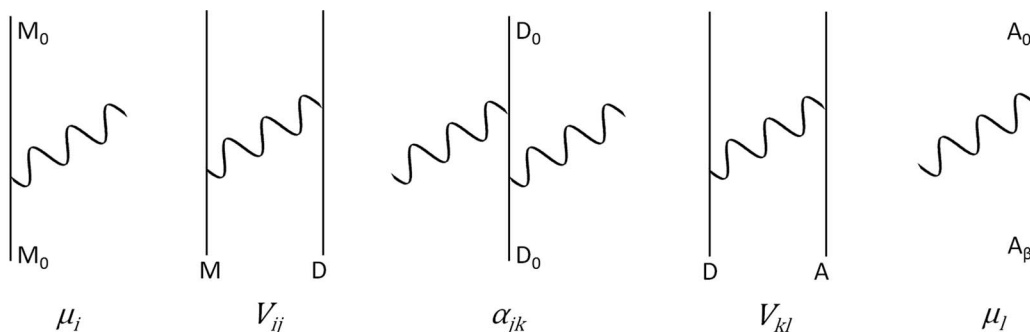


FIG. 5. The five factors of M_{MDA} , each corresponding to a coupling element illustrated by one part of Fig. 3. Reproduced by permission from D. L. Andrews and J. S. Ford, Proc. SPIE **8459**, 84590C (2012). Copyright 2012 SPIE.

phenomenologically

$$\alpha_{ij}^{X_r X_0}(-k'; k) = - \sum_{X_r} \left[\frac{\mu_i^{X_r X_r} \mu_j^{X_r X_0}}{E_{r0}^X - \hbar c k - i \hbar c \gamma_r^X} + \frac{\mu_j^{X_r X_r} \mu_i^{X_r X_0}}{E_{r0}^X + \hbar c k' \pm i \hbar c \gamma_r^X} \right]. \quad (7)$$

A variety of physically distinct features and processes contribute to spectral damping, including the finite lifetime of electronic excited states, the manifold of vibrational states typically associated with each of those states, and a finite radiation linewidth. The inclusion of damping in polarizability formulas is essentially pragmatic and phenomenological,³⁰ it is impossible to reconcile any rigorous form with the demands of time-reversal invariance, due to the non-Hermitian nature of the Hamiltonian for an implicitly non-conservative system. The sign of the damping correction on the dominant, potentially resonant term in the polarizability (the first term in Eq. (7)) proves uncontroversial, and leads to a Lorentzian lineshape. Different arguments support varying conclusions on the sign and magnitude of the damping in the anti-resonant term,^{31–33} but the results cannot be experimentally differentiated. Accordingly, the sign for the damping correction to the anti-resonant term can be left unspecified, and has no bearing on the following development: the correction to this term can be effectively omitted.

The sum in Eq. (6) over all transitional states r of chromophore D is now expressible as the relevant transition polarizability, $\alpha_{bc}^{D_0 D_\alpha}(-k; 0)$. Also, the factors involving \mathbf{R}_{MD} and \mathbf{R}_{DA} are expressible in terms of the rank-two electro-dynamical coupling tensor which is ubiquitous in two-body RET work.²⁰ Using the notation $\hat{R}_j \equiv R_j/R$,

$$\begin{aligned} V_{ij}(k; \mathbf{R}) &\equiv (4\pi\epsilon_0)^{-1} (\nabla^2 \delta_{ij} - \nabla_i \nabla_j) R^{-1} \exp(ikR) \\ &= (4\pi\epsilon_0)^{-1} R^{-3} \exp(ikR) \{ (\delta_{ij} - 3\hat{R}_i \hat{R}_j) \\ &\quad - ikR(\delta_{ij} - 3\hat{R}_i \hat{R}_j) - k^2 R^2 (\delta_{ij} - \hat{R}_i \hat{R}_j) \}. \end{aligned} \quad (8)$$

Expressions (7) and (8) permit a concise and expedient statement of the quantum amplitude for the MDA configuration. Equation (6) is thus finally cast as

$$\begin{aligned} M_{MDA} &= \mu_i^{M_0 M_0} V_{ij}(0; \mathbf{R}_{MD}) \alpha_{jk}^{D_0 D_\alpha}(-k; 0) \\ &\quad \times V_{kl}(k; \mathbf{R}_{DA}) \mu_l^{A_\beta A_0}. \end{aligned} \quad (9)$$

B. Other coupling configurations

Figure 5 shows that each of the five factors of Eq. (9) corresponds to one of the coupling phenomena which together comprise the MDA energy transfer process as illustrated by the Feynman diagram of Fig. 3. The spatial indices i, j, k, l continue to correspond to the transition dipole moments of the four transitions, the vertices of the Feynman diagram. The arguments of the tensor V_{kl} indicate that it describes the transfer of energy $\hbar ck$ over the distance \mathbf{R}_{DA} via the coupling interaction. The tensor V_{ij} connects the third body to the RET system, but zero energy is exchanged between M and D.³⁴

Building on Eq. (9), formulae for the other two three-body configurations may be derived by substitution of variables. The quantum amplitudes for the DAM configuration and for the DMA configuration thus evaluate as

$$\begin{aligned} M_{DAM} &= \mu_i^{D_0 D_\alpha} V_{ij}(k; \mathbf{R}_{DA}) \alpha_{jk}^{A_\beta A_0}(0; k) \\ &\quad \times V_{kl}(0; \mathbf{R}_{AM}) \mu_l^{M_0 M_0}, \end{aligned} \quad (10)$$

$$\begin{aligned} M_{DMA} &= \mu_i^{D_0 D_\alpha} V_{ij}(k; \mathbf{R}_{DM}) \alpha_{jk}^{M_0 M_0}(-k; k) \\ &\quad \times V_{kl}(k; \mathbf{R}_{MA}) \mu_l^{A_\beta A_0}. \end{aligned} \quad (11)$$

Equations (10) and (11) may be constructed from (9) by comparing Fig. 6 with Fig. 3.

The latter of these, DMA, has been considered in recent work by Salam;²² our work extends the analysis by additionally including the influence of static dipole coupling with M – that coupling being with the donor in the form of coupling represented as MDA, and with the acceptor in the case of DAM. In general, one should also account for the second-order process of two-body RET, not involving any M. This has quantum amplitude expressible in the same formalism as

$$M_{DA} = \mu_i^{D_0 D_\alpha} V_{il}(k; \mathbf{R}_{DA}) \mu_l^{A_\beta A_0}. \quad (12)$$

C. Quantum interference

It is a central feature of the quantum electro-dynamical method utilized here that the analysis directly secures results for physical measurables – here, the rate of excitation transfer. The measurable rate of the transfer of excitation energy between two chromophores D and A in the presence of a

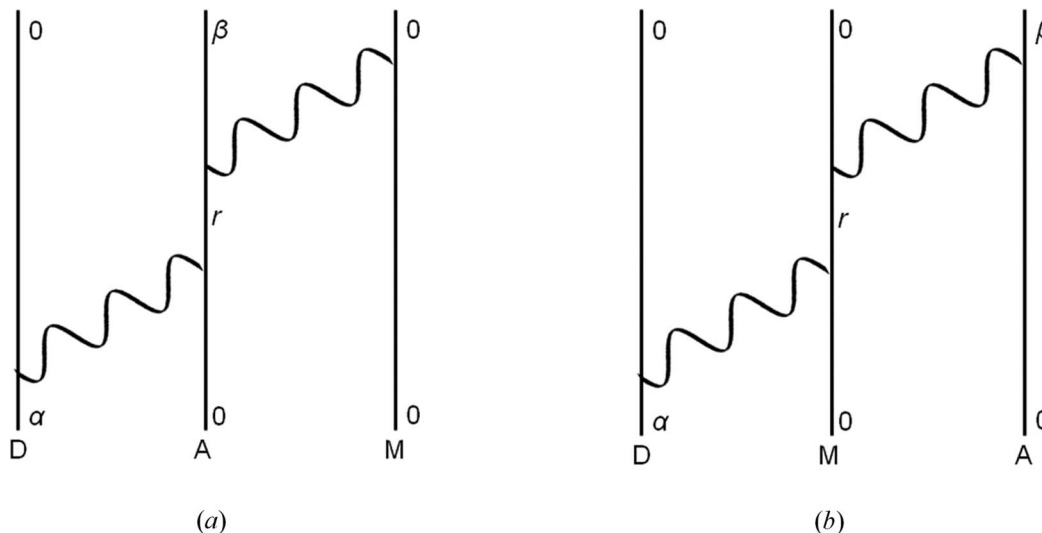


FIG. 6. Feynman diagrams for the other two three-body configurations: (a) DAM configuration; (b) DMA configuration. These have the same structure as Fig. 3 but with different chromophores and state labels. Reproduced by permission from D. L. Andrews and J. S. Ford, Proc. SPIE **8459**, 84590C (2012). Copyright 2012 SPIE.

passive molecule M is predicted by the Fermi rule, Eq. (2), as proportional to the square modulus of a quantum amplitude for that process. The four quantum amplitude results derived above all describe this same process via different intermediate stages, so may be summed to deliver the general quantum amplitude. The square modulus of the sum over four amplitudes results in ten complex product terms

$$\begin{aligned}
 \Gamma_{FI} &= 2\pi \hbar^{-1} \rho_F |M_{DA} + M_{MDA} + M_{DAM} + M_{DMA}|^2 \\
 &= 2\pi \hbar^{-1} \rho_F \{ |M_{DA}|^2 \\
 &\quad + 2\text{Re}(\bar{M}_{DA} M_{DMA}) + |M_{MDA}|^2 \\
 &\quad + 2\text{Re}(\bar{M}_{DA} M_{DAM}) + 2\text{Re}(\bar{M}_{MDA} M_{DAM}) + |M_{DAM}|^2 \\
 &\quad + 2\text{Re}(\bar{M}_{DA} M_{MDA}) + 2\text{Re}(\bar{M}_{MDA} M_{DMA}) \\
 &\quad + 2\text{Re}(\bar{M}_{DAM} M_{DMA}) + |M_{DMA}|^2 \}. \quad (13)
 \end{aligned}$$

There is considerable complexity in each of the terms in this expression, and in order to most readily elicit the associated physical significance it is both appropriate and expedient to introduce some simplifying assumptions about the physical system. We therefore focus on the case where the transition dipole moments $\mu^{D_o D_\alpha}$ and $\mu^{A_\beta A_o}$ are parallel, together defining a direction that will be designated the z -axis, also assuming that the three molecules are separated by a distance significantly less than k^{-1} , though necessarily beyond significant wavefunction overlap. One immediate consequence is that Eq. (8) reduces to

$$\lim_{kR \rightarrow 0} V_{ij}(k; \mathbf{R}) = (4\pi\epsilon_0)^{-1} R^{-3} (\delta_{ij} - 3\hat{R}_i \hat{R}_j) \quad (14)$$

and each of the coupling tensors in Eqs. (9)–(12) now takes this real form, independent of the wavenumber, with the appropriate displacement argument. It can be anticipated that the significance of molecules M displaced beyond this near-zone region will be insignificant, in light of the monotonic decline in the interaction strength with distance.

To proceed further, aiming to identify the dependence of the energy transfer on the positional and electronic properties of the component M – without the encumbrance of secondary vector and tensor considerations – we now conduct an average over all molecular orientations of M. In Fig. 7, the ten distinct contributions to Eq. (13) are identified, along with the specific factors involving the orientation of M in each term; the application of each relevant tensor average is denoted below by chevron brackets. It then emerges that four of these terms disappear because they involve an isotropic tensor average $I^{(n)}$ of odd rank n .

Specifically, terms involving the fully index-antisymmetric average $I^{(3)}$ are index-contracted with physical tensor components with exchange symmetry in one index pair; the other terms involve $I^{(1)}$ which is intrinsically zero. Details are given in Ref. 35. As is apparent, the non-vanishing terms fall into two groups of three; one group involves M in the role of static dipole (the inner three in Fig. 7), whereas M enters the other three terms only through its scattering polarizability if at all. Physically, the significance is that the former terms will be enhanced for molecules M that are intrinsically highly polar, whereas the latter set of terms are of greater importance in the case of highly polarizable species. Furthermore, it is clear that the term $\text{Re}(\bar{M}_{DA} M_{DMA})$ signifies the leading correction to $|M_{DA}|^2$, the most important contribution in which M plays a role, and $|M_{DMA}|^2$ is one of four equally higher-order corrections. In consequence, we can focus on $\text{Re}(\bar{M}_{DA} M_{DMA})$, which entails the real part of a product of four complex factors

$$\begin{aligned}
 \text{Re}(\bar{M}_{DA} M_{DMA}) &= \mu_i^{D_o D_\alpha} \mu_m^{D_o D_\alpha} \mu_l^{A_\beta A_o} \mu_n^{A_\beta A_o} \\
 &\quad \times \text{Re}[V_{ij}(k; \mathbf{R}_{DM}) V_{kl}(k; \mathbf{R}_{MA}) \\
 &\quad \times \bar{V}_{mn}(k; \mathbf{R}_{DA}) \alpha_{jk}^{M_o M_o}(-k; k)]. \quad (15)
 \end{aligned}$$

Recognizing that indices i , l , m , and n are now limited to z , and interpreting the results according to Eqs. (12)–(15)

| | | | | |
|-----|----------------------------------------------------------------------------------------------------------------------|---------------------------------------------------------------------------------------------------------------------------------------|---------------------------------------------------------------------------------------------------------------------------------------|------------------------------------------------------------------------------------------------------------------------|
| DA | $\langle M_{DA} ^2 \rangle$ $\equiv M_{DA} ^2$ | | | |
| MDA | $\langle \text{Re}(\bar{M}_{DA} M_{MDA}) \rangle$ $\propto \langle \mu_i^{M_o M_o} \rangle \propto I^{(1)}$ | $\langle M_{MDA} ^2 \rangle$ $\propto \langle \mu_i^{M_o M_o} \mu_j^{M_o M_o} \rangle \propto I^{(2)}$ | | |
| DAM | $\langle \text{Re}(\bar{M}_{DA} M_{DAM}) \rangle$ $\propto \langle \mu_i^{M_o M_o} \rangle \propto I^{(1)}$ | $\langle \text{Re}(\bar{M}_{MDA} M_{DAM}) \rangle$ $\propto \langle \mu_i^{M_o M_o} \mu_j^{M_o M_o} \rangle \propto I^{(2)}$ | $\langle M_{DAM} ^2 \rangle$ $\propto \langle \mu_i^{M_o M_o} \mu_j^{M_o M_o} \rangle \propto I^{(2)}$ | |
| DMA | $\langle \text{Re}(\bar{M}_{DA} M_{DMA}) \rangle$ $\propto \langle \alpha_{ij}^{M_o M_o} \rangle \propto I^{(2)}$ | $\langle \text{Re}(\bar{M}_{MDA} M_{DMA}) \rangle$ $\propto \langle \mu_i^{M_o M_o} \alpha_{jk}^{M_o M_o} \rangle \propto I^{(3)}$ | $\langle \text{Re}(\bar{M}_{DAM} M_{DMA}) \rangle$ $\propto \langle \mu_i^{M_o M_o} \alpha_{jk}^{M_o M_o} \rangle \propto I^{(3)}$ | $\langle M_{DMA} ^2 \rangle$ $\propto \langle \alpha_{ij}^{M_o M_o} \alpha_{kl}^{M_o M_o} \rangle \propto I^{(4)}$ |
| | DA* | MDA* | DAM* | DMA* |

FIG. 7. Rotational average of M applied to the terms of Eq. (13). The six emphasized terms are non-vanishing.

finally gives

$$\begin{aligned}
 \langle \Gamma_{FI} \rangle &= \frac{2\pi \rho_F}{\hbar} [|M_{DA}|^2 + 2\langle \text{Re}(\bar{M}_{DA} M_{DMA}) \rangle + \dots] \\
 &= \frac{\rho_F}{48 \pi^2 \hbar \varepsilon_0^3} |\mu^{D_o D_o}|^2 |\mu^{A_\beta A_o}|^2 R_{DA}^{-3} (1 - 3\hat{R}_{DAz}^2) \\
 &\quad \times \{ 6\pi \varepsilon_0 R_{DA}^{-3} (1 - 3\hat{R}_{DAz}^2) \\
 &\quad + R_{DM}^{-3} R_{MA}^{-3} [1 - 3\hat{R}_{DMz}^2 - 3\hat{R}_{MAz}^2 \\
 &\quad + 9\hat{R}_{MAz} \hat{R}_{DMz} (\hat{R}_{MA} \cdot \hat{R}_{DM})] \text{Re}(\text{Tr} \alpha^{M_o M_o}(-k; k)) \\
 &\quad + \dots \}, \tag{16}
 \end{aligned}$$

where all variables involving M are collected together in one term. Clearly, the key factors are the position, orientation, and the trace polarizability of the passive chromophore. The result, Eq. (16) can be interpreted as the rate for RET between donor and acceptor, modified by the presence of the passively interacting medium. In view of the sharp diminution of this influence with the displacement of M from D and A, the terms in Eq. (16) that refer to M can be interpreted as applying specifically to the M unit closest to the energy transfer pair. Indeed, M need not be restricted to a location beyond the region occupied by the donor and acceptor – this model can account for the influence of a non-participant molecule located within that region, acting as an integral part of the energy transfer system.

The complicated interplay of factors associated with the relative positions and orientations of the three chromophores makes it impossible to give a simple general prescription for M producing amplification of the energy transfer rate. However, the analysis does provide clear rules that can be applied to any specific geometry. Take, for example, the case $(\hat{R}_{MA} \cdot \hat{R}_{DM}) = 0$, satisfied when M is situated at any point on the surface of a notional sphere, on which the positions of the donor and acceptor represent opposite poles. It then follows from Eq. (16) that amplification will then occur provided

$$1 + 9\hat{R}_{DAz}^2 (\hat{R}_{DMz}^2 + \hat{R}_{MAz}^2) > 3(\hat{R}_{DAz}^2 + \hat{R}_{DMz}^2 + \hat{R}_{MAz}^2). \tag{17}$$

This is based on the fact that the trace polarizability factor $\text{Re}(\text{Tr} \alpha^{M_o M_o}(-k; k))$ in Eq. (16) must be positive, since our mechanism specifically requires that the energy being transferred corresponds to an optical frequency that is redshifted from the primary absorption band of the species M. The above inequality evinces supplementary conditions for the case under consideration: amplification of the transfer rate is assured if the principal axis of D and A (the z -axis) is oriented orthogonal to the DMA plane.

IV. DISPERSION BEHAVIOR

We have identified that the role of non-polar chromophores M in modifying resonance energy transfer hinges on the polarizability tensor $\alpha_{ij}^{M_o M_o}(-k; k)$, which is the time-symmetric inert scattering tensor of the molecule M, as defined by Eq. (7). As we have seen, the inclusion of an imaginary damping correction in each energy denominator, accounting for finite line shape, has the result that the tensor is regarded as a complex quantity. The two-event process that is mediated by M has three physical features which specify it as a simple scattering: there are only two interaction events within a system satisfying overall energy conservation with the radiation field; the final state M_F is identical to M_0 such that M undergoes no overall transition; the transition dipole moments μ are entirely real (which is always possible, given a suitable choice of basis). It follows from these points that $k = k'$ and $\mu_i^{M_0 M_r} \mu_j^{M_r M_0} = \mu_j^{M_0 M_r} \mu_i^{M_r M_0}$. Also, the intermediate states r form a complete set of stationary states for the molecule.

We now focus on the important possibility of a stationary excited state of the species M being near to resonance with the energy $\hbar ck$; we designate this particular near-resonant intermediate state as ε . In implementing the sum over states in the explicit formula (7), the chosen ε may be extracted from the sum over r , with the substitution $\Delta_\varepsilon \equiv E_{\varepsilon 0}/\hbar c - k$ representing the energy separation from resonance: the exact resonance condition is $\Delta_\varepsilon = 0$. The damped result for molecule M is then

$$\alpha_{ij}^{M_0M_0}(-k; k) = \frac{-1}{\hbar c} \left\{ \mu_i^{M_0M_\varepsilon} \mu_j^{M_\varepsilon M_0} \left[\frac{\Delta_\varepsilon + i\gamma_\varepsilon}{\Delta_\varepsilon^2 + \gamma_\varepsilon^2} + \frac{\Delta_\varepsilon + 2k \mp i\gamma_\varepsilon}{(\Delta_\varepsilon + 2k)^2 + \gamma_\varepsilon^2} \right] \right. \\ \left. + \sum_{r \neq \varepsilon} \mu_i^{M_0M_r} \mu_j^{M_r M_0} \left[\frac{k_{r0} - k + i\gamma_r}{(E_{r0}^M / \hbar c - k)^2 + \gamma_r^2} + \frac{k_{r0} + k \mp i\gamma_r}{(E_{r0}^M / \hbar c + k)^2 + \gamma_r^2} \right] \right\}. \quad (18)$$

In this form, it is trivial to separate the real and imaginary parts. The near-resonance case of Eq. (18) is found by neglecting all $r \neq \varepsilon$ terms and also the anti-resonant ε term, as they become negligible in comparison to the relevant resonance term. In this case, the real trace polarizability that features in Eq. (16) is therefore given by

$$\text{Re}(\text{Tr} \alpha_{ij}^{M_0M_0}(-k; k)) = -(\hbar c)^{-1} \mu^{M_0M_\varepsilon} \mu^{M_\varepsilon M_0} \frac{\Delta_\varepsilon}{\Delta_\varepsilon^2 + \gamma_\varepsilon^2}. \quad (19)$$

From this point, we can identify special types of behavior that will arise under particular conditions, determined by the interplay of factors associated with the electronic properties intrinsic to M, and the amount of energy being transferred between D and A. Simplifications, based on a truncated Taylor series expansion, arise under two cases of particular physical interest

$$\text{Re}(\text{Tr} \alpha_{ij}^{M_0M_0}(-k; k)) \cong \begin{cases} -(\hbar c)^{-1} \mu^{M_0M_\varepsilon} \mu^{M_\varepsilon M_0} [\Delta_\varepsilon^{-1} - \gamma_\varepsilon^2 \Delta_\varepsilon^{-3}], & (\gamma_\varepsilon \ll |\Delta_\varepsilon|) \\ -(\hbar c)^{-1} \mu^{M_0M_\varepsilon} \mu^{M_\varepsilon M_0} [\Delta_\varepsilon \gamma_\varepsilon^{-2} - \Delta_\varepsilon^3 \gamma_\varepsilon^{-4}], & (\gamma_\varepsilon \gg |\Delta_\varepsilon|) \end{cases}. \quad (20)$$

These functions of k describe the wavelength-dependence of the passive molecule Ms influence on RET, through Eq. (16). Since, in that equation, it is only the polarizability that varies with k , the Clausius-Mossotti relation may be used to express this dependence as an optical dispersion behavior. Specifically, a relationship can be established with the variation in wavelength of the refractive index n of a medium comprised entirely of species M. The general Clausius-Mossotti relation delivers the linear polarizability of species M present in number density N , as a function of the refractive index n of pure M

$$\alpha = 3N^{-1} \frac{n^2 - 1}{n^2 + 2}. \quad (21)$$

The prior assumption that there is an isotropic distribution of orientations for molecule M is consistent with the physically reasonable case for the associated polarizability itself to exhibit an isotropic form, with each diagonal element expressible as the scalar given by Eq. (21). While such isotropy holds, the real trace tensor that features in Eq. (16) is expressible as triple the Clausius-Mossotti result. Treating

the variable n^2 as complex

$$\text{Re}(\text{Tr} \alpha_{ij}^{M_0M_0}(-k; k)) = 3\text{Re}\alpha = 9N^{-1} \frac{\text{Re}(n^2)^2 + \text{Re}(n^2) + \text{Im}(n^2)^2 - 2}{[\text{Re}(n^2) + 2]^2 + \text{Im}(n^2)^2}, \quad (22)$$

n is now interpreted as the refractive index of a medium consisting of M, within which RET between isolated molecules D and A occurs – assuming the latter species is present in low concentration. We thus use the dispersion relationship to link the bulk refractive index of a material M to the effect that the presence of its molecules have upon RET.

Cast in this form, the result has a greater capacity for interpretation than the conventional method, in which the coupling tensor V_{ij} , in a medium-modified quantum amplitude from Eq. (12), is redefined to involve the medium's refractive index.³⁶ This has been the basis for work analyzing the protein scaffolding of photosynthetic systems as a polarizable environment.^{37,38} The two approaches are far from equivalent – interpreting $\alpha_{jk}^{M_0M_0}(-k; k)$ in Eq. (15) to be independent of n and giving the V tensors the prefactor $(n^2 + 2)^2/9n^2$ results in a rate dependence on n that does not replicate Eq. (22). Our analysis has addressed a physically different scenario, identifying effects associated with a specific local chromophore. Since M is identified as the closest medium molecule, it is clearly inconsistent to model the space between the RET pair and M as being filled with matter that modifies coupling via its non-unity refractive index.

V. DISCUSSION

This research opens up substantial opportunities to reevaluate the standard physical interpretations of known RET mechanisms, and to refocus the direction of ongoing mathematical exploration of the theory. In particular, Eq. (16) is representative of results arising from quantum interference between amplitudes for different energy transfer mechanisms. When RET systems are of sufficiently high symmetry, it is possible to discern which contributions are relevant for consideration in specific materials because the various interference terms are subject to different combinations of spectroscopic selection rule; but with low-symmetry systems, all possible quantum interferences may participate in the observed form of energy transfer. Our aim here has been to develop the physical principles based on a chosen exemplar, extending previous, less detailed accounts of similar form that focused on the short-range influence of a non-polar third body on energy transfer efficiency.^{22,29}

At the molecular level, the effects of a surrounding medium on RET has been pursued in terms of dispersion in the scattering polarizability of neighboring molecules, related to the surroundings' refractive index through the Clausius-Mossotti equation. The notions of compositional fraction and refractive index are bulk concepts, so it must be cautioned that any analysis which models the surrounding medium as a featureless homogenous matrix will fail to register the detailed electronic effects of ancillary non-spherical molecules in close vicinity to the RET chromophores. Our analysis bridges the gap between three photon-exchanging molecules and a refractive bulk material by assuming that the RET chromophores are present in low concentration and taking the medium to be isotropic in the sense that the orientations of its molecules are averaged. The DMA configuration has functional similarities to a DA energy transfer that is modified by the "screening" influence of a polarizable solvent, as has been identified in other work treating the medium molecules collectively as a surrounding fluid.^{39,40} Nonetheless, the medium is here considered as comprising discrete molecules with characteristic electronic properties. The case where M contributes as a polar species, through its static electric dipole moment μ^{00} , can be interpreted physically as signifying an influence on the electromagnetic coupling between the donor and the acceptor, through the static electric field which the dipole produces. Conversely, for systems in which M primarily interacts as a polarizable chromophore via its dynamic molecular polarizability, the mechanism for modifying the form of energy transfer is one in which M intervenes through its acquiring an induced electric dipole. Clearly, the degree of ionic and covalent character in the molecular constitution of the passive chromophore will help determine which properties are most relevant.

Measurements of RET usually focus on rates, and typically the efficiency of RET can be gauged by one of two means: either by detection of fluorescence from the acceptor, or by monitoring a reduction in spontaneous fluorescence from the donor.⁴¹ To observe the effect of a third party, as in the theory we have presented, suggests the need to compare such results in systems that accommodate, or fail to accommodate, such other chromophores in the immediate vicinity. At this stage, it becomes a matter of experimental strategy, and the results for a particular set of materials will inform on the role and significance of the species acting in the role of chromophore M.

To conclude, we note that there are numerous physical systems in which the operation of resonance energy transfer mechanisms may be approximately described as involving three close chromophores, two of which exchange a quantum of excitation while the third influences the rate without changing its energy state; copious examples can be found in the operation of natural photosynthetic systems, as well as in biomimetic multi-chromophore dendrimers used for artificial light harvesting.^{8,42} In terms of synthetic materials, further examples arise in connection with the strategic placement of off-resonant chromophores in quantum dot assemblies.⁴³ These can all provide for the active modification and all-optical control of key optical effects, not limited to RET. The results we have secured should support applications in light

harvesting energy materials, optical switching, data processing, communication, and computation, through the achievement of new methods for optically controlled transmission.

ACKNOWLEDGMENTS

We gratefully acknowledge helpful comments from Dr. David Bradshaw. J.S.F. is supported by the Engineering and Physical Sciences Research Council (U.K.).

- ¹R. E. Blankenship, *Molecular Mechanisms of Photosynthesis* (Blackwell, Oxford, 2002).
- ²N. P. A. Huner, K. E. Wilson, E. Miskiewicz, D. P. Maxwell, G. R. Gray, and M. K. A. A. G. Ivanov, in *Energy Harvesting Materials*, edited by D. L. Andrews (World Scientific, NJ, 2005), pp. 97–142.
- ³G. D. Scholes, G. R. Fleming, A. Olaya-Castro, and R. v. Grondelle, *Nat. Chem.* **3**, 763–774 (2011).
- ⁴J. L. Herek, N. J. Fraser, T. Pullerits, P. Martinsson, T. Polivka, H. Schee, R. J. Cogdell, and V. Sundstrom, *Biophys. J.* **78**, 2590–2596 (2000).
- ⁵D. L. Andrews, S. P. Li, J. Rodriguez, and J. Slota, *J. Chem. Phys.* **127**, 134902 (2007).
- ⁶G. D. Scholes and G. R. Fleming, *J. Phys. Chem. B* **104**, 1854–1868 (2000).
- ⁷B. Valeur, *Molecular Fluorescence* (Wiley-VCH, Weinheim, 2002), p. 248.
- ⁸D. L. Andrews, "Optical energy harvesting materials," in *Introduction to Complex Mediums for Optics and Electromagnetics*, edited by W. S. Weiglhofer and A. Lakhtakia (SPIE, Bellingham, Washington, 2003), pp. 141–163.
- ⁹F. Barigelletti and L. Flamigni, *Chem. Soc. Rev.* **29**, 1–12 (2000).
- ¹⁰Z. Tan, R. Kote, W. N. Samaniego, S. J. Weininger, and W. G. McGimpsey, *J. Phys. Chem. A* **103**, 7612–7620 (1999).
- ¹¹V. Balzani, P. Ceroni, A. Juris, M. Venturi, S. Campagna, F. Puntoriero, and S. Serroni, *Coord. Chem. Rev.* **219–221**, 545–572 (2001).
- ¹²J. Barber, *Philos. Trans. R. Soc. London, Ser. A* **365**, 1007–1023 (2007).
- ¹³K. Schulten, in *Simplicity and Complexity in Proteins and Nucleic Acids*, edited by H. Frauenfelder, J. Deisenhofer, and P. G. Wolynes (Dahlem University Press, 1999), pp. 227–253.
- ¹⁴A. Adronov and J. M. J. Fréchet, *Chem. Commun.* **2000**, 1701–1710.
- ¹⁵S.-C. Lo and P. L. Burn, *Chem. Rev.* **107**, 1097–1116 (2007).
- ¹⁶G. R. Fleming, G. S. Schlau-Cohen, K. Amarnath, and J. Zaks, *Faraday Discuss.* **155**, 27–41 (2012).
- ¹⁷T. Förster, *Ann. Phys.* **437**, 55–75 (1948).
- ¹⁸D. L. Andrews and B. S. Sherborne, *J. Chem. Phys.* **86**, 4011–4017 (1987).
- ¹⁹D. L. Andrews, *Chem. Phys.* **135**, 195–201 (1989).
- ²⁰D. L. Andrews and D. S. Bradshaw, *Eur. J. Phys.* **25**, 845–858 (2004).
- ²¹D. Beljonne, C. Curutchet, G. D. Scholes, and R. J. Silbey, *J. Phys. Chem. B* **113**, 6583–6599 (2009).
- ²²A. Salam, *J. Chem. Phys.* **136**, 014509 (2012).
- ²³D. P. Craig and T. Thirunamachandran, *Molecular Quantum Electrodynamics*, 1st ed. (Academic Press, London, 1984).
- ²⁴A. Salam, *Molecular Quantum Electrodynamics: Long-range Intermolecular Interactions* (Wiley, Hoboken, NJ, 2010).
- ²⁵L. Mandel and E. Wolf, *Optical Coherence and Quantum Optics* (Cambridge University Press, Cambridge, 1995).
- ²⁶D. L. Andrews and P. Allcock, *Optical Harmonics in Molecular Systems* (Wiley-VCH, Weinheim, 2002).
- ²⁷R. D. Jenkins, D. L. Andrews, and L. C. D. Romero, *J. Phys. B* **35**, 445–468 (2002).
- ²⁸E. W. Weisstein, *From MathWorld—A Wolfram Web Resource*, see <http://mathworld.wolfram.com/HasseDiagram.html>.
- ²⁹G. J. Daniels and D. L. Andrews, *J. Chem. Phys.* **117**, 6882–6893 (2002).
- ³⁰D. L. Andrews, S. Naguleswaran, and G. E. Stedman, *Phys. Rev. A* **57**, 4925–4929 (1998).
- ³¹D. L. Andrews, L. C. Dávila Romero, and G. E. Stedman, *Phys. Rev. A* **67**, 055801 (2003).
- ³²P. R. Berman, R. W. Boyd, and P. W. Milonni, *Phys. Rev. A* **74**, 053816 (2006).
- ³³P. W. Milonni, R. Loudon, P. R. Berman, and S. M. Barnett, *Phys. Rev. A* **77**, 043835 (2008).
- ³⁴D. L. Andrews and J. S. Ford, *Proc. SPIE* **8459**, 84590C (2012).
- ³⁵D. L. Andrews and T. Thirunamachandran, *J. Chem. Phys.* **67**, 5026–5033 (1977).

- ³⁶G. Juzeliūnas, *Chem. Phys.* **198**, 145–158 (1995).
- ³⁷C. Curutchet, J. Kongsted, A. Muñoz-Losa, H. Hossein-Nejad, G. D. Scholes, and B. Mennucci, *J. Am. Chem. Soc.* **133**, 3078–3084 (2011).
- ³⁸J. Adolphs and T. Renger, *Biophys. J.* **91**, 2778–2797 (2006).
- ³⁹G. D. Scholes, C. Curutchet, B. Mennucci, R. Cammi, and J. Tomasi, *J. Phys. Chem. B* **111**, 6978–6982 (2007).
- ⁴⁰S. Caprasecca, C. Curutchet, and B. Mennucci, *J. Chem. Theory Comput.* **8**, 4462–4473 (2012).
- ⁴¹B. Valeur and M. N. Berberan-Santos, *Molecular Fluorescence: Principles and Applications*, 2nd ed. (Wiley-VCH, Weinheim, 2013).
- ⁴²G. D. Scholes and G. Rumbles, *Nature Mater.* **5**, 683–696 (2006).
- ⁴³T. Kawazoe, K. Kobayashi, and M. Ohtsu, *Appl. Phys. Lett.* **86**, 103102 (2005).